A SPECTROSCOPIC SURVEY FOR BINARY STARS
IN THE GLOBULAR CLUSTER NGC 5053

Lin Yan[1] and J. G. Cohen

Department of Astronomy, MS 105-24

California Institute of Technology; Pasadena, CA 91125

Email: lyan@eso.org, jlc@astro.caltech.edu

arXiv:astro-ph/9607116v1   23 Jul 1996

---

[1] Present address: European Southern Observatory; Karl-Schwarzschild-Str. 2; D-85748 Garching b. München; Germany

ABSTRACT

We carried out a radial velocity survey for spectroscopic binaries in the low density globular cluster NGC 5053. Our sample contains a total of 77 cluster member giant and subgiant stars with visual magnitudes of 14.5−18.6. Of these 77 stars, 66 stars have on average of 3−4 measurements with a total of 236 velocities. A typical velocity error per measurement is $\sim$3 km s^{-1}. The stars in our sample are spatially distributed from the cluster center out to 10 arcminutes in radius (4.5 core radii). Among these 66 stars with multiple velocity measurements, we discovered 6 spectroscopic binary candidates. Of these six candidates, one was discovered as a binary previously by Pryor et al. (1991) and candidate ST is a binary with a very short-period of three to five days. We obtained three possible orbital solutions for binary candidate ST by fitting its radial velocity data. These orbital solutions are consistent with star ST being a cluster member, although its spectrum has much stronger MgI triplet absorption lines than that of a typical low-metallicity giant star.

Using a Monte-Carlo simulation method, we estimated the fraction of binary systems which may have been missed from our detection due to unfavorable orbital configurations. With our survey, the binary discovery efficiency is 29% for systems with 3 d $\leq$ P $\leq$ 10 yr, 0.125 $\leq$ q $\leq$ 1.75 and eccentric orbits (0 $\leq$ e $\leq$ 1). This yields a binary frequency of 29%. We also applied Kolmogorov-Smirnov (K-S) tests to the cumulative distributions of maximum velocity variations from the actual measurements and the synthetic velocity data. The results from these tests are consistent with 21−29% binary population with 3 d $\leq$ P $\leq$ 10 yr, 0.125 $\leq$ q $\leq$ 1.75 in NGC 5053. The hypothesis of a binary frequency in NGC 5053 higher than 50% is rejected with a confidence level higher than 85%.

The binary frequency in NGC 5053 derived from our survey is somewhat higher than estimates for other clusters by various surveys. This is perhaps related to the fact that NGC 5053 is relatively dynamically young compared to other clusters. We also argue that the binary population in globular clusters is not significantly deficient compared to binaries in other stellar environments such as open clusters, or to field and low metallicity halo stars.

1. INTRODUCTION

Recently it has been realized that a primordial binary frequency as small as 3% can fundamentally change the dynamical evolution of an entire globular cluster (Heggie & Aarseth 1992). Mass segregation caused by two body relaxation in a cluster essentially transfers "heat" (stellar kinetic energy) from the cluster core to the "cooling" edges, while simultaneously pushing the cluster towards higher central concentration (*gravothermal collapse*). The process of gravothermal collapse can be greatly modified by a binary star

population (Gao *et al.* 1991; Heggie & Aarseth 1992; McMillan & Hut 1994; Vesperini & Chernoff 1994). Gravitational binding energy in binary stars can be extracted and converted into kinetic energy during encounters with other stars. The extracted energy can supply a central heat source to stave off or reverse gravothermal collapse.

There is considerable observational evidence that binary stars do exist in globular clusters (see the detailed review by Hut *et al.* 1992). Discoveries of low-mass X-ray binaries (LMXB) in globular clusters (Grindlay *et al.* 1984) first hinted that a primordial binary population could exist in globular clusters, although the formation of LMXBs doesn't necessarily require the pre-existing binary populations. Indisputable evidence came from the discovery of long-period binary millisecond pulsars in low density globular clusters during the late 80's and the early 90's. Among a total of ∼40 millisecond pulsars in globular clusters, ∼12 of them are actually in binary systems. Furthermore, two of these binary millisecond pulsars —discovered in the *low density clusters* M 4 and M 53— have *periods as long as 200−300 days* (McKenna *et al.* 1988; Kulkarni *et al.* 1991). Binaries with such long periods cannot be formed through single star-star tidal capture. In fact, PSR 1640-26 in M 4 is a triple system. These two long period millisecond pulsars either have to be formed by star-binary and binary-binary encounters, or their progenitors are primordial binary stars.

Recent direct searches for spectroscopic and short-period eclipsing binaries have discovered many binary systems and binary candidates in globular clusters (Pryor *et al.* 1992; Côte *et al.* 1994; Mateo *et al.* 1990; Yan & Mateo 1994; Yan & Reid 1995). One of the drivers behind these efforts is to understand many apparently different phenomena in globular clusters which may be intimately related to binary star population. For example, such phenomena include blue stragglers, color/stellar gradient in the cores of post-core-collapsed clusters (Djorgovski & King 1986), X-ray sources and numerous "recycled" radio pulsars (Phinney 1992; Phinney 1995). The discovery of short-period eclipsing binaries among both blue straggler stars and main-sequence stars (Mateo *et al.* 1990; Kaluzny and Krzeminski 1993; Yan & Mateo 1994; Yan & Reid 1995) suggests that the short-period binaries may be the progenitors of blue stragglers. Mass transfer/merger among stars in binary systems and stellar encounters involving binary stars are important processes for the formation of blue stragglers. Also, numerous X-ray sources and radio pulsars in globular clusters can be easily explained in terms of binary systems containing degenerate stars.

While mounting evidence, direct or indirect, has suggested the existence of both short and long period binary stars in globular clusters, the binary frequency and binary period distributions are very poorly determined. This has been the major source of uncertainty in the theoretical modeling the role of binaries in the evolution of globular clusters. For binaries with periods in the range of 10 days to 10 years, the direct way to determine the binary frequency is to systematically measure radial velocity variations in individual stars

of a globular cluster. Technically, only recently with the advent of high resolution multi-object spectrographs on 4-meter class telescopes did it become possible for the first time to sample a large number of stars and to obtain multi-epoch observations with a reasonable amount of telescope time. With telescopes smaller than the Keck 10-meter telescope, we are limited to bright red giants and subgiants even in the closest globular cluster. These bright low metallicity giant stars have smaller masses and larger radii compared to the field G-type stars. Consequently, a binary system containing such a bright giant star is difficult to detect since the system tends to have a long period and small radial velocity variations.

All of the existing radial velocity surveys of binary stars in globular clusters generally were done among the bright giant stars (Gunn & Griffin 1979; Pryor, Latham & Hazen 1988; Côte et al. 1994). The first radial velocity survey with high precision was done by Gunn & Griffin (1979) in the globular cluster M 3. They obtained a total of 85 velocity measurements for 33 giant stars with V magnitudes 12−14. They failed to find any binary candidates among the non-pulsating stars and concluded that binaries with separations between 0.3−10 AU (periods between 0.1 years and 30 years) were much rarer in globular clusters than in the field Population I stars. In 1988, combining Gunn & Griffin's data in M 3 with new MMT observations, Pryor et al. produced a larger dataset containing 111 giant stars, each with 3 multiple measurements. They found one binary candidate, which later was confirmed as a system with a period of 7.3 years. Recently, Côte et al. (1994) published a similar survey in the globular cluster NGC 3201. A total of 786 velocities were obtained for 276 giant stars with V magnitudes of 11.0−16.5 over a total timespan of 6 years. They found 2 good binary candidates, plus 13 possible candidates. The derived binary frequency from both surveys is roughly $5\% - 18\%$ for systems with $0.1 \text{ yrs} \leq P \leq 10 \text{ yrs}$ and $0.1 \leq q \leq 1.0$, depending on orbital eccentricities.

With the advent of the Norris Multi-fiber Spectrograph on the 200 inch telescope at the Palomar observatory, we carried out a radial velocity survey for spectroscopic binary stars in the globular cluster NGC 5053. Our survey was designed to reach much fainter stars than previous surveys. It is thus sensitive to binary systems with much shorter periods, and much larger radial velocity variations. The object sample in our survey consists of 77 cluster member giant and subgiant stars in the globular cluster NGC 5053 with visual magnitudes in the range of 14.2−18.6. We have obtained 6 epochs of observations of these 77 stars in a total timespan of 3 years. Compared to the previous radial velocity survey made in the same cluster by Pryor et al (Pryor, Schommer & Olszewski 1991), our survey samples more than twice as many stars and goes almost three magnitude fainter. Our survey is sensitive to binary systems with periods as short as 3 days. For potential binaries in our sample, a maximum radial velocity variation as large as 116 kms^{-1} is possible for an edge-on circular orbit with M_1 and M_2 of $0.8 M_{\odot}$ and $0.5 M_{\odot}$ respectively. Our velocity measurement error varies from star to star, but typically is about 3 km s^{-1}, which is

somewhat worse than in previous surveys (We discuss in detail the velocity measurement errors and related problems in §2.2). However, the smaller radii of the stars in our sample compensates for this disadvantage. In addition, our sample stars are less luminous and don't have radial velocity variations on a scale of 8 kms^{-1} caused by intrinsic atmospheric motions found among bright giant stars by previous surveys (Gunn & Griffin 1979; Lupton, Gunn & Griffin 1987; Pryor *et al.* 1988).

The globular cluster NGC 5053 is an ultra-low density cluster with a half-mass relaxation timescale of $\sim$ 8 Gyr (Djorgovski 1992), comparable to the Hubble timescale. This suggests that this cluster is barely dynamically relaxed, and the spatial and period distribution of its primordial binary population has not been significantly altered by two-body relaxation processes. Moreover, the long relaxation timescale indicates that in this cluster the binary destruction by star-binary and binary-binary encounters is not important. However, one disadvantage imposed on our survey is that NGC 5053 is a very metal poor cluster with [Fe/H] of -2.2, and thus the spectra from its stars have weaker metal absorption lines than metal rich objects.

2. THE SURVEY

2.1. Observations

All of the observations were made with the Norris Multi-fiber Spectrograph on the Hale 5.0m telescope at the Palomar observatory. The Norris Spectrograph is a fiber-fed multi-object spectrograph which is mounted at the Cassagrin focal plan of the telescope (Hamilton *et al.* 1993). It has a total of 176 fibers, and each fiber has a 1.6 arcsecond diameter aperture. The small diameter of the fiber aperture implies that the effective throughput of the spectrograph is very sensitive to seeing conditions, especially for stellar objects, as in our case. The fibers are located in two opposing banks of equal number. The minimum separation between two fibers is $\sim$ 16 arcsecond, which is the major limitation for sampling more stars in globular clusters. The spectrograph covers a field of view of 20×20 square arcminutes.

We obtained a total of 6 epochs of observations of a sample of 77 cluster member stars with a total timespan of 3 years. The summary of all observations is tabulated in Table 1. The first four epochs of observations in 1992 and 1993 were taken with a 1024×1024 pixels CCD and the field of view of 10×10 square arcminutes. The last two epochs of observations in 1994 were taken with a more sensitive and larger CCD with 2048x2048 pixels. These observations therefore had wider wavelength coverage and sampled more stars. Thus some of the stars in our sample have more velocity measurements than others. Also notice that the total exposure time for the primary field in NGC 5053 varies from one epoch to another due to changes in the amount of available observing time and the observing conditions. For some epochs, we could not obtain any observations for the second field in the same

cluster. This is one of the causes for the variations of velocity measurement errors for the same star at different epochs.

During all observations, we used a 1200 groove/mm grating centered around 5000 Å. The resulting spectral scale is $\sim$ 0.65 Å/pixel, corresponding to the velocity scale of $\sim$39 km s^{-1}pixel^{-1}. The spectral resolution of the observations is around 2.5$-$3 Å. With a cross-correlation technique, we should be able to measure any velocity shift larger than one tenth of a pixel, $i.e.$ 4 km s^{-1}. The poor resolution in the April 1994 observing run was due to bad collimator focus caused by a mechanical problem in the spectrograph.

To make accurate velocity measurements, in all our observations we took comparison Thorium-Argon spectra both before and after each object exposure to calibrate out any spectrograph flexure. Dome flats were taken immediately after each setup to flatfield the object spectra. We also obtained some exposures of the twilight sky to check the spectrograph velocity zero-point shifts between different nights and also between different observing runs. Depending on the observing conditions and the amount of time we had during each run, we observed at least the primary field and sometimes the secondary field in NGC 5053. Since it is relative velocity variations which we need to measure accurately in the search for spectroscopic binaries, we chose about 10 giant stars brighter than 13 magnitude in the globular cluster M 13 to serve as the velocity standards. These giant stars were chosen from the sample in the radial velocity survey by Lupton, Gunn & Griffin (1987). The typical velocity error in their survey is $\sim$1 km s^{-1}. One advantage of using these stars is that we were able to obtain all their spectra with a single exposure.

2.2. Data Reduction

Our data were reduced using IRAF.[1] After the images were trimmed and corrected for bias, all of the object spectra, including sky expsoures, were identified, traced and extracted using APALL task in the IRAF package SPECRED. An optimal extraction algorithm was used to produce one-dimensional spectra for all stars. The dome-flat spectra from all fibers were extracted and averaged. A low-order polynomial was used to fit the averaged dome-flat spectrum. The flatfield spectra were obtained by normalizing all dome-flat spectra with the single fitted spectrum. The CCD sensitivity variations at small scales in all object spectra were taken out by dividing them with the corresponding flatfield spectra.

Figures 1(a) and 1(b) show spectra of the same star with a signal-to-noise ratio of $\sim$15, taken in 1992 and 1994 respectively. Signal-to-noise ratios of our spectra vary within a large range, but the typical value of a continuum is around 10. The spectra taken in 1994 have the wavelength coverage of 4700Å$-$5800Å, and consequently include very strong sky

---

[1] IRAF is distributed by the National Optical Astronomy Observatories, which are operated by the Association of Universities for Research in Astronomy, Inc., under contract to the National Science Foundation.

emission lines such as [OI] 5577Å, HgI 5461Å, the Hg doublet 5791Å, and the NaD doublet 5893Å. To obtain good sky subtraction, we corrected the variations of throughput from fiber to fiber. The correction for each fiber was estimated by dividing the integrated flux in the sky emission line HgI5461Å with the average flux of the same line from all fibers. The most useful absorption lines for doing radial velocity cross-correlation, H_β4861Å and the MgI triplet at 5167, 5173 and 5184Å, are outside the strong sky emission line region. Residuals of sky emission lines in the sky-subtracted spectra do not have a big effect on the velocity measurement. In the cases of large residuals from the sky subtraction, we simply mask off the regions with sky lines. Throughput correction was not necessary for spectra taken in 1992 since there are not many strong sky emission lines in the range of 4710Å−5300Å. Figure 1(c) shows the spectrum of the radial velocity standard II-76 in the globular cluster M 13.

All wavelength calibrations were done only with a set of isolated lines. Typically, we used 3rd order polynomial fitting and obtained an rms error in the dispersion solution less than 0.04 Å, which corresponds to a velocity error of less than 2 kms^{-1}. Each stellar spectrum was wavelength calibrated with its own comparison spectra which were taken through the same fiber before and after the star exposure. To make sure spectra taken through different fibers and in different nights have the same wavelength scale, we cross-correlated every wavelength calibrated thorium-argon spectrum against all the other Th-Ar spectra. With care in the calibration procedure, we were able to keep the relative shift between all Thorium-Argon spectra under 2 kms^{-1}.

The object spectra were dispersion corrected and binned into log wavelength. Radial velocities for all stars in the sample were obtained with a cross-correlation technique (Tonry & Davis 1979). Each object spectrum was cross-correlated with the template spectra of radial velocity standards. We used the task FXCOR in RV package of IRAF to obtain radial velocity measurements.

2.3. Radial Velocities

We have obtained a total of 247 new radial velocities for 77 cluster member giant and subgiant stars in the globular cluster NGC 5053. Of the 77 cluster member stars, 66 stars have multiple radial velocity measurements and are suitable for a binary search. Therefore, we will concentrate only on those 66 stars. Table 2 lists photometry, astrometry and 247 radial velocities for those 77 stars in NGC 5053. The columns record, from left to right, the star's identification names, right ascension and declination in the epoch of 1950.0, the radial distance from the cluster center in arcseconds, the heliocentric Julian date (+244000 in days) of the observation, the heliocentric radial velocity at the date and its corresponding uncertainty in kms^{-1}, the number of observations, the weighted mean radial velocity and the external velocity error in a single measurement estimated from the dispersion about the mean, the chi-square for the observations and the probability of

obtaining a chi-square at least this large purely due to measurement errors. The final two columns give the star's magnitude and (B − V) color. Some of the photometry listed in Table 2 are from Sandage et al (Sandage, Katem & Johnson 1977) and the rest are our measurements. To distinguish the stars originally identified in the SKJ paper from the new stars we selected, we combined the same names SKJ used with the prefix S. Table 2 is published in the CD-ROM supplement to this journal due to its large size. Anybody who is interested in Table 2 could also contact LY directly.

In Table 2, the second and any subsequent lines under each object report the radial velocities and the internal errors at the corresponding heliocentric Julian dates. For a combined set of velocities, we calculated χ^2 and the weighted mean velocity (for details, see Duquennoy & Mayor 1991). The χ^2 value represents the radial velocity variability over the timespan of three years. To evaluate the significance of the variations represented by χ^2, we calculated the probability of having a χ^2 at least this large purely due to chance fluctuations with a Gamma function Q(0.5ν, 0.5χ^2), here ν is the number of the degree of freedom. Reasonable limits of χ^2 probability for identifying significant variations are 0.01− 0.001.

The velocities tabulated in Table 2 are the radial velocities of stars in NGC5053 relative to star II-76 in M 13. The globular clusters M 13 and NGC 5053 have cluster systematic velocities of about −246.4 km s^{-1} and 43 kms^{-1} respectively (Pryor & Meylan 1993). Figure 2 shows the histogram of all relative velocities tabulated in Table 2 including non-cluster member velocities. With only cluster members and excluding the variable stars, the mean relative velocity is 291.0 kms^{-1} and the standard deviation is 3.7 kms^{-1}.

2.4. Error Analyses

As shown in Table 1, we usually took multiple exposures of the same set of stars in a single observing run. We measured velocities using individual spetcra as well as using the sum of these individual spetcra of the same star. For some faint stars, summation of all exposures within a single observing run is required in order to have enough signal to measure velocities.

One problem with summation is that it works fine for almost all types of potential binaries in our sample *except* binaries with periods of a few days. The shortest period for a binary allowed by the sizes of stars in our sample is ∼3 days. In the case of an edge-on circular orbit with $M_1 = 0.8M_\odot, M_2 = 0.5M_\odot$, the expected peak-to-peak radial velocity variation is ∼113 km s^{-1}. Obviously the binaries with such an orbital configuration can be easily identified by inspecting the velocities measured during the same observing run. We found only one binary candidate ST with radial velocity (individual measurements) variations larger than 30 km s^{-1} over two days. This star is a strong candidate for a short-period spectroscopic binary (see §3.1 for detailed discussion of this system). However, the binaries with periods of a few days and *near face-on* orbits will not show large radial

velocity variations during a single observing run. Summation of spectra will smear out velocity variations of this type of binaries and we can not distinguish them from single stars. The problem is partly inherent for this type of binaries, and partly due to the noisy spectra of the faint stars in our survey. Fortunately, the probability of having this particular type of binaries in our sample is very small ($\leq \sim 2\%$). The final result of the survey should not be significantly affected by this limitation.

Making a realistic estimate of the internal error for each radial velocity measurement is crucial for identifying the radial velocity variables. The internal velocity errors are evaluated as follows. The quality of a cross-correlation can be characterized by a quantity R (for the definition of R, see Tonry & Davis 1979). The larger R is, the more accurate the velocity is. The value of R reflects the signal-to-noise ratio of the object spectrum as well as how well the object spectrum matches with the template spectrum. With this definition of R, the internal error is calculated as $\sigma = \frac{\sigma_0}{1+R}$, here σ_0 is a constant which can be estimate with our data.

The method we used to estimate σ_0 is similar to the one described in Pryor et al. (1988) and Vogt et al. (1995). We took the velocity difference Δv between each pair of velocities for those stars with multiple measurements. Then $\sigma_0 = \frac{\Delta v}{[(1+R_1)^{-2}+(1+R_2)^{-2}]^{1/2}}$, here R_1 and R_2 are the Tonry & Davis values for velocity v_1 and v_2 respectively. If velocity errors have a Gaussian distribution, σ_0 is equal to the standard deviation of a normal distribution produced by the above equation. The second way is to compute the velocity difference Δv between the weighted mean velocity and a given measurement v_i. Then σ_0 is $\frac{(v_i-\bar{v})}{[(1+R_i)^{-2}+(\sum(1+R_i)^{-2}]^{1/2}}$. Figure 3 shows the σ_0 distribution. It is roughly gaussian and the standard deviation σ_0 is 44.7 kms^{-1} for the April 1992 observation. For all observed objects, Figure 4 is the plot of the internal velocity error versus R of each velocity measurement. A separate σ_0 was estimated for each observing run. With the derived σ_0, we got a total χ^2 of 185.1 for 196 degrees of freedom for all velocities in our sample excluding non-members and potential variables. The probability of a χ^2 larger than this is 0.68, which is acceptable.

For all stars in our sample, velocity errors listed in Table 2 are calculated using σ_0 estimated with the above method and R values from the summed spetcra. A typical error is ~ 3 km s^{-1}, but the worst is as large as 10 km s^{-1}. This large variation is partly due to the instrinsic luminosity differences between stars in our sample, and partly because some stars were observed more frequently than others. In addition, the accuracy of fiber positioning is different from star to star and from one observing run to another. With non-uniform velocity measurement errors, it is dangerous to use only the velocity variations between different epochs to represent the true velocity variabilities due to orbital motion of binary stars. The more effective way of selecting binary candidates is to calculate χ^2 of all velocity measurements and the probability of obtaining a χ^2 value larger than observed

9

by chance.

The velocity zero-point   shifts between different epochs were examined by cross-correlating spectra of bright stars in M 13. The twilight spectra taken in several epochs were also used to estimate the velocity zero-point shifts. We didn't find any significant velocity zero-point shifts between different epochs.

3. RESULTS

3.1. Spectroscopic Binary Candidates

Using the criterion that a binary candidate must have a velocity χ^2 such that the probability of obtaining a χ^2 larger than this value by chance is less than 0.01, we identified 6 spectroscopic binary candidates among a sample of 66 cluster member stars. The χ^2 probabilities of these six binary candidates indicate that their radial velocity variations are significant over the timespan of 3 years. Of these 6 binary candidates, star S5 was previously found as a binary candidate in the Pryor et al. survey (1991) and star ST is a binary candidate with a very short period and a large-amplitude velocity variation. Table 3 lists these six spectroscopic binary candidates. Figure 5 is a cluster color-magnitude diagram, in which the solid triangles represent five of the six binary candidates discovered by our survey, candidate ST is marked separately with a solid square and the hollow circles show the three brighter binary candidates discovered in the Pryor et al. (1991) survey. Figures 6(a)−(e) are the detailed finding charts of the 6 binary candidates. The star is $318.1''$ away from the cluster center and located in an isolated environment, as shown in Figure 6(e). (B-V) color and V magnitude of binary candidate ST are are fairly consistent with those of the cluster member stars.

We fit the velocity data and obtain the orbital solutions for star ST. However, due to the small number of velocity measurements, the orbital solution for star ST is not unique. Figure 7 shows the three possible solutions. In the figure, P is the period, V_0 the center-of-mass velocity, K the amplitude of the orbital velocity and e the eccentricity. These possible orbital solutions and its photometric color suggest that star ST is a cluster member. However, the spectrum of this star has a much stronger $Mg\lambda5177$ triplet absorption line compared to that of a low-metallicity giant star. The analyses of the $Mg\lambda5177$ line strength verses the photometric color (for the details of the method, see Faber *et al.* 1985; Gorgas *et al.* 1993) indicate that the spetcrum of star ST is similar to that of a metal-rich dwarf. But considering that star ST is a very short-period spectroscopic binary, we conclude the parcularity of its absorption line strength could result from the possible interaction between the two components of the binary system; star ST is probably a cluster member. We should point out that if star ST is a cluster member giant and if its period is around three to five days, this binary system must be on the verge of Roche lobe overflow since the primary star has a fairly large radius.

3.2. Modeling the binary frequency[2]

In any spectroscopic survey for binary stars, the probability of detecting a binary depends not only on the binary frequency, but also on a set of unknown binary orbital parameters such as period, eccentricity, mass ratio, orbital phase and inclination angle of the binary system. Unfavorable binary orbital configurations would cause a fraction of binary systems to be missing from our detection sample. Thus, to properly interpret the measurements in our survey, we use Monte-Carlo simulation methods to generate a large number of simulated radial velocity data sets and compare them with the measured radial velocities. We calculate from the synthetic data sets the fraction of binaries missed in our survey, then correct the observed binary frequency. We applied the same criterion used in the survey to the synthetic data for identifying binary candidates. This criterion is that the probability of obtaining a χ^2 larger than observed by chance has to be less than 0.01.

An additional statistical method is to use a Kolmogorov-Smirnov (K-S) test to compare the cumulative distributions of maximum velocity differences for the real data to the mean distribution determined from a large number of simulated data sets. This method has been used in several surveys, such as Harris & McClure (1983), Pryor et al. (1988) and Côte et al. (1994). We will discuss in detail the applicability of this method to our data in section §4.3.

3.2.1. The binary models

The simulation code for generating synthetic radial velocities was generously provided to us by Dr. C. Pryor. Some modifications have been made during our calculations. In solving Kepler's equations, we made the following assumptions: the binary period, mass ratio and eccentricity distribution functions were taken as the ones in Duquennoy and Mayor (1991, thereafter DM), which were derived for G-type dwarf stars in the solar neighbourhood. The orbital longitude ω and the initial orbital phase were drawn randomly between 0 and 2π from a uniform distribution. $\cos(i)$, where i is the inclination angle of the orbital plan to the line of sight, was chosen randomly from 0 to 1 with a uniform distribution. Of course, the mass of the primary is assumed to be $0.8M_\odot$. Our survey is sensitive to binaries with the minimum and maximum periods of 3 days and 10 years respectively, and with mass ratio larger than 0.125.

The effect of mass transfer was considered in our simulations by eliminating the binary system whenever the two stars get closer than the critical Roche lobe radius. The radius of the primary was calculated from its photometry using the Revised Yale Isochrones (Green, Demarque & King 1987). Figure 8 shows the stellar radius versus absolute visual

---

[2] Here the binary frequency is defined as the ratio of the number of binary candidates to the total number of "stars", here "stars" includes both single stars and binary stars; and a binary is counted as "one star".

magnitude (reddening corrected) for the stars in our sample. In Figure 8, the solid line is calculated for the metallicity of -2.2 from the models, the solid triangles represent the stars in our sample with the adopted distance modulus $(m - M)_{V0}$ of 16.08 magnitude and $E(B - V)$ of 0.06 magnitude (Fahlman, Richer & Nemec 1991). Also shown in the figure with the hollow squares are the empirical radii for giants in the clusters M 92 by Cohen, Frogel and Persson (1987) based on broad-band infrared photometry and narrow-band CO and H_2O indices. The globular cluster M 92 has a metallicity [Fe/H] of -2.2, very similar to NGC 5053.

We didn't consider the effect of asymptotic giant branch in our calculations because in our sample less than 24% of stars are above the Horizontal branch.

3.2.2. The binary frequency

To convert the binary discovery fraction of 0.084 (5.5/65.5, giving candidate ST 0.5 weight due to some ambiguity of its cluster membership) to the true binary frequency f_b, we estimate the incompleteness correction using Monte-Carlo simulations. This correction is also called the binary discovery efficiency D_b, which is defined as the fraction of the "discovered" binaries in the synthetic velocity data if we assume all 66 stars as binary systems. Radial velocities of each binary were calculated using the binary models described in §3.2.1 at the actual observation dates. Velocity noises were drawn randomly from Gaussian distributions with the mean of zero and standard deviations of the *real velocity measurement errors*. By applying the same binary identifying criterion used in the survey, we obtained the fraction of "discovered" binaries in the simulated data. Figures 9(a)−(b) show the binary discovery efficiency D_b as a function of period P in days for the binary models with circular orbits and with eccentricity distribution $f(e) = 1.5\sqrt{e}$ respectively. Notice that each data point in the plots is the mean of 1000 simulation tries. Here we assume the primary star in a binary system to have $0.8M_\odot$, and a mass ratio q (defined as M_2/M_1) in the range of 0.125 to 1.75. This implies that the secondary could be anything from a $0.1M_\odot$ low mass star to a $1.4M_\odot$ heavy neutron star. In both plots, the solid triangles and dots represent simulations with and without the effect of mass transfer respectively. It is clearly shown in the figures that the biasing of the discovered binary orbits by the size of the giants is significant at the short period end. This bias is higher for stars with brighter magnitudes, which is the major reason that the previous surveys could not detect any binary with period shorter than 40 days.

In the case of non-zero eccentricity orbits, the average binary discovery efficiency is about 29% for binaries with 3 days $\leq P \leq$ 10 years and $0.125 \leq q \leq 1.75$. For binaries with the same period and mass ratio range, the inferred true binary frequency f_b is $0.084/D_b$, i.e. 29%. In the case of circular orbits, the corresponding binary frequency for systems with periods and mass ratios in the same ranges is 26%. The discovery efficiency varies as the limits of binary period and mass ratio change. A binary with a very low mass companion

is usually difficult to detect even if the period is short. For instance, the primary star in a binary with a period of 100 days shows a maximum radial velocity change of 10 km s^{-1} in the case of an edge-on circular orbit and $M_1 = 0.8M_\odot$, $M_2 = 0.1M_\odot$. If we choose the sensitivity limits of our survey as 3 days $\leq P \leq 10$ years and $0.3 \leq q \leq 1.75$, the binary discovery efficiency is 35% and 37% for the binary models with non-circular and circular orbits respectively. The corresponding binary frequency f_b in the cluster is 24% and 23% respectively.

4. DISCUSSION

4.1. An alternative period distribution function in globular clusters

The binary frequency estimated above depends on the adopted period distribution in the simulations. An alternative period distribution has a constant number of binaries per unit logarithmic period interval. This so called "flat" period distribution is a crude representation of the survey by Abt & Levy (1976). The "flat" distribution produces more short-period binaries and less long period ones for 3 d $\leq P \leq 10$ yr than the DM period distribution. Obviously, it also gives a somewhat higher binary discovery efficiency for our survey. Specifically, with an average discovery efficiency of 36% derived from the "flat" distribution, we obtained a binary frequency of 23% for systems with 3 d $\leq P \leq 10$ yr, $0.125 \leq q \leq 1.75$ and $f(e) = 1.5\sqrt{e}$. Similarly in the case of circular orbits, the inferred binary frequency is 21%. For the mass ratio range of $0.3 \leq q \leq 1.75$, the derived binary frequencies are 19% and 22% for circular and eccentric orbits respectively. The binary frequency derived by using the "flat" period distribution is smaller than using the DM period distribution in the simulations. The binary period distribution in globular clusters perhaps bears more similarities with ones in open clusters and among Pop. II low metallicity halo stars. Many extensive programs of studying binary stars in open clusters and among low metallicity halo stars (Carney & Latham 1987; Latham *et al.* 1988, 1992) should shed light on the properties of binary populations in globular clusters.

4.2. The effect of stellar encounters

We did not take into account the effect of stellar encounters in our calculations. This effect can alter the shape of the primordial distributions of binary orbital elements in globular clusters. As briefly discussed in §2.1, this effect is not significant in very low density clusters such as NGC 5053 since the cluster half-mass relaxation timescale is comparable to a Hubble timescale T_h. However, of the eight globular clusters in which radial velocity surveys for binary stars have been carried out by various groups (Hut *et al.* 1992), six have cluster central relaxation timescales T_{rh} much shorter than T_h of 14 Gyr. These six clusters include M 3, M 13, 47 Tuc, M 2, M 71 and NGC 3201, where T_{rh} is in the range of 10^8 to 10^9 yrs. NGC 3201 and M 71 have particularly short T_{rh} of only 100 million years in spite of their apparent low central densities.

It is a rather complicated problem to characterize quantitatively the change in the primordial period distribution due to dynamical evolution. A tremendous amount of theoretical computations have been devoted to this subject (Phinney & Sigurdsson 1991; McMillan & Hut 1994; Sigurdsson & Phinney 1995). The detailed N-body simulations (McMillan, Hut & Makino 1991) show that binary-binary encounters are a very effective binary-destruction process. Most binary destruction occurs within a few core radii of the cluster center. In addition, some binaries can be ejected to the outer parts of a cluster due to large recoil during binary-binary encounters in the core. Thus, in dynamically evolved clusters such as M 71 it is perilous to assume the field period distribution.

Although it is premature to draw any comprehensive conclusions about the binary frequency dependence on the dynamical properties of globular clusters, it is illuminating to compare the results from various surveys for binary stars in different globular clusters. As first pointed out by Pryor et al (1991; Hut *et al.* 1992), the binary discovery rate in NGC 5053 is notably higher than other clusters where binary searches have been carried out. The result of our survey appears to further support Pryor's conclusion. This is perhaps associated with the fact that NGC 5053 is a dynamically young cluster.

4.3. Kolmogorov-Smirnov (K-S) tests

As Harris & McClure (1983) first pointed out, small number statistics are important in estimating binary frequencies in globular clusters. Subsequently a sophisticated and quantitative statistical method —the Kolmogorov-Smirnov test— has been employed in many surveys. K-S tests were applied to the cumulative distributions of maximum velocity difference obtained from both simulated and real data. A K-S statistic is useful for *rejecting* the null hypothesis that two data sets are drawn from the same parent distribution.

We applied K-S statistics to our measured velocities and the simulated data. In Table 4, we tabulated the confidence level at which the null hypothesis of the simulated data and real data drawn from the same distribution is accepted. K-S tests show that the binary frequency in NGC 5053 is close to 25%, and the hypothesis that the binary frequency is higher than 50% is rejected with confidence higher than 85%. However, it is noticed in Table 4 that with our data K-S tests are not very effective in *rejecting* the cases with different binary frequencies. This problem results from some of the large errors in our velocity measurements. As described previously, the synthetic data were generated using the actual velocity errors. The corresponding cumulative distribution of maximum velocity variation is primarily controlled by a few large errors. K-S tests have been applied more effectively by Pryor et al. (1989) and Côte et al. (1994) to their data with the radial velocity errors are as small as 1 kms^{-1}. They have derived a binary frequency in the range of 10% to 20% for binaries with $0.1 \text{ yr} \leq P \leq 20 \text{ yr}$.

REFERENCES

Abt, H.A. & Levy, S.G., 1976, ApJS, 30, 273

Carney, B.W. & Latham, D.W., 1987, AJ, 93, 116

Cohen, J.G., Frogel, J.A., & Persson, S.E., 1978, ApJ, 222, 165

Côte, P., Welch, D.L., Fischer, P., Da Costa, G.S., Tamblyn, P., Seitzer, P., & Irwin, M.J., 1994, ApJS, 90, 83

Djorgovski, S. & King, I.R., 1986, ApJL, 305, L61

Djorgovski, S., 1992, in *Structure and Dynamics of Globular Clusters*, ed. by S.G. Djorgovski and G. Meylan, (San Fransisco: ASP), 50, 357

Duquennoy, A. & Mayor, M., 1991, A&A, 248, 485

Faber, S.M., Friel, E.D., Burstein, D. & Gaskell, C.M., 1985, ApJS, 57, 711

Fahlman, G.G., Richer, H.B. & Nemec, J., 1991, ApJ, 380, 124

Gao, B., Goodman, J., Cohn, H., Murphy, B., 1991, ApJ 370, 567

Gorgas, J., Faber, S.M., Burstein, D., Gonzalez, J.J., Courteau, S. & Prosser, C., 1993, ApJS, 86, 153

Green, E.M., Demarque, P. & King, C.R., 1987, *The Revised Yale Isochrones and Luminosity Functions*, Yale University Observatory.

Grindlay, J.E., Hertz, P., Steiner, J.E., Murray, S.S. & Lightman, A.P., 1984, ApJ, 282, L13

Gunn, J.E. & Griffin, R.F., 1979, AJ, 84, 752

Kaluzny, J. & Krzeminski, W., 1993, MNRAS, 264, 785

Kulkarni, S.R., Anderson, S.B., Prince, T.A. & Wolszczan, A., 1991, Nature, 349, 47

Hamilton, D., Oke, J.B., Carr, M.A., Cromer, J., Harris, F.H., Cohen, J.G., Emery, E. & Blakee, L., 1993, PASP, 105, 1308

Harris, H.C. & McClure, R.D., 1983, ApJL, 265, L77

Heggie, D.C. & Aarseth, S.J., 1992, MNRAS, 257, 513

Hut, P., McMillan, S.L.W., Goodman, J., Mateo, M., Phinney, E.S., Richer, H.B., Verbunt, F. and Weinberg, M., 1992, PASP, 104, 981

Latham, D.W., Mazeh, T., Stefanik, R.P., Davis, R.J., Carney, B.W., Krymolowski, Y., Laird, J.B., Torres, G. & Morse, J.A., 1992, AJ, 104, 774

Latham, D.W., Mazeh, T., Carney, B.W., McCrosky, R.E., Stefanik, R.P. & Davis, R.J., 1988, AJ, 96, 567

Lupton, R.H., Gunn, J.E. & Griffin, R.F., 1987, AJ, 93, 1114

Mateo, M., Harris, H.C., Nemec, J. and Olszewski, E.W., 1990, AJ, 100, 469.

McKenna, J. & Lyne, A.G., 1988, Nature, 336, 226

McMillan, S.L.W. & Hut, P., 1994, ApJ, 427, 793

McMillan, S.L.W., Hut, P. & Makino, J., 1991, ApJ, 372, 111

Phinney, E.S., 1992, Philos. Trans. R. Soc. Lond., A, 341, 39

Phinney, E.S. & Sigurdsson, S., 1991, Nature, 349, 220

Phinney, E.S., 1996, in *The Origins, Evolution, and Destinies of Binary Stars in Clusters*, ed. Eugene F. Milone, (San Francisco: ASP), 90, in press

Pryor, C.P., Latham, D.W. & Hazen, M.L., 1988, AJ, 96, 123

Pryor, C.P., Meylan, G. 1993, in *Structure and Dynamics of Globular Clusters*, ed. by S.G. Djorgovski and G. Meylan, (San Francisco: ASP), 50, 357

Pryor, C., Schommer, R.A. & Olszewski, E.W. 1991, in *The Formation and Evolution of Star Clusters*, ed. Janes, (San Fransisco: ASP), 13, 121

Sandage, A.R., Katem, B. & Johnson, H.L., 1977, AJ, 82, 389

Sigurdsson, S. & Phinney, E.S., 1995, ApJS, 99, 609

Tonry, J. & Davis, M., 1979, AJ, 84, 1511

Vesperini, E. & Chernoff, D.F., 1994, ApJ, 431, 231

Vogt, S., Mateo, M., Olszewski, E.W. & Keane, M.J., 1995, AJ, 109, 151

Yan, L. & Mateo, M., 1994, AJ, 108, 1810

Yan, L. & Reid, N. I., 1995, MNRAS, 279, 751

FIGURE CAPTIONS:

Figure 1: Figures 1(a) and 1(b) show spectra of star LY014 taken in 1992 and 1994. Figure 1(c) is the spectrum of star II-76 in M 13 which serves as a radial velocity standard.

Figure 2: The histogram of all relative radial velocities measured in our survey including non-members of the cluster stars. Each bin is 1.55km s^{-1} wide. The majority of the stellar radial velocities distributed around the cluster relative velocity. Non-members of the cluster stars are clearly distinguished from the member stars by their radial velocities. Also notice that the dispersion around the mean radial velocity is only 3.7 kms^{-1} excluding the measurements from non-member stars and binary candidates.

Figure 3: The distribution of σ_0 derived from our data. See the text for the detailed discussion.

Figure 4: The plot shows the velocity error versus the Tonry & Davis value R. The envelope of the velocity errors in the figure is roughly proportional to $\propto R^{-1}$, as described in Tonry & Davis (1979).

Figure 5: This shows the cluster color-magnitude diagram, where the solid triangles show five of the six binary candidates discovered in this survey, the solid square indicates the short-period binary candidate ST, and the open circles represent the candidates found previously by Pryor et al. (1991).

Figure 6: The detailed finding charts for the 6 binary candidates. All objects are plotted relative to the position with RA (1950)=13:14:5.070 and DEC (1950)=17:56:38.00. The axes are in units of arcsecond, the north and the east are indicated in the plot.

Figure 7: The plots show the three possible orbital solutions fitted to the available data.

Figure 8: This is a plot of the stellar radius vs. the luminosity for stars in globular clusters. The curve is generated using the Revised Yale Isochrones and Luminosity Functions (Green *et al.* 1987) with Y= 0.2 and an age of 15 Gyr. The solid traingles represent the stars in our sample, and open squares are the measurements for stars in M 92 by Cohen et al. (1987).

Figure 9: Figure shows the binary discovery efficiency D_b as a function of period P (in days) for two different binary models. In both panels the solid triangles and the solid dots represent the simulations with and without considering the mass transfer effect respectively. Note that each data point in the plots is the mean of 1000 simulation tries.

TABLE 1

Summary of Observing Log

Date (UT)	Object	Exp. Time (sec)	$\Delta\lambda$ (Å)	Resolution (Å)	Weather conditions
7/4/1992	NGC 5053	3×3000	4710−5310	2.5	clear, 1.3″ seeing
7/4/1992	M 13	1×900	4710−5310	2.5	clear, 1.3″ seeing
8/4/1992	NGC 5053[2]	3×3000	4710−5310	2.5	cloudy, 1.3″ seeing
8/4/1992	M 13	1×900	4710−5310	2.5	cloudy, 1.3″ seeing
25/5/1992	NGC 5053	2×3000	4710−5310	2.5	cloudy, 1.5″ seeing
26/5/1992	NGC 5053	3×3000	4710−5310	2.5	clear, 1.5″ seeing
26/5/1992	M 13	1×900	4710−5310	2.5	clear, 1.5″ seeing
16/4/1993	NGC 5053	1×3000	4710−5310	2.5	cloudy, 1.5″ seeing
16/4/1993	M 13	1×900	4710−5310	2.5	cloudy, 1.5″ seeing
21/5/1993	NGC 5053	1×2515	4710−5310	2.5	cloudy, 1.5″ seeing
21/5/1993	M 13	1×900	4710−5310	2.5	cloudy, 1.5″ seeing
11/4/1994	NGC 5053	3×3000	4700−5800	3.0	clear, 1.2″ seeing
11/4/1994	M 13	2×700	4700−5800	3.0	clear, 1.2″ seeing
12/4/1994	NGC 5053	3×3000	4700−5800	2.5	cloudy, 1.5″ seeing
12/4/1994	M 13	3×900	4700−5800	3.0	cloudy, 1.5″ seeing
12/4/1994	NGC 5053[2]	4×3000	4700−5800	3.0	cloudy, 1.5″ seeing
8/5/1994	NGC 5053	3×3000	4700−5800	2.5	cloudy, 1.3″ seeing
8/5/1994	M 13	1×600	4700−5800	2.5	cloudy, 1.3″ seeing
10/5/1994	NGC 5053	2×3000	4700−5800	2.5	clear, 1.2″ seeing
10/5/1994	M 13	3×600	4700−5800	2.5	clear, 1.5″ seeing
10/5/1994	NGC 5053[2]	2×3000	4700−5800	3.0	cloudy, 1.5″ seeing
10/5/1994	M 13	1×900	4700−5800	2.5	clear, 1.3″ seeing

Notes: NGC 5053[2] is the second field we observed in the same cluster. In M 13 several bright giant stars were observed to serve as the radial velocity standards. The radial velocities of these stars have been accurately measured by Lupton, Gunn and Griffin (1987). The third column in the table gives the number of exposure times the time of a single exposure, *i.e.* the total exposure time. The spectral resolution in April 1994 is larger than other runs due to problems with the collimator focus in the Norris spectrograph during that observing run. The CCD spectral scale is 0.65 Å pixel^{-1} for all of the observations.

TABLE 4

KOLMOGOROV-SMIRNOV PROBABILITIES
FOR MODEL ACCEPTANCE

	3d $\leq$ P $\leq$ 10yr 0.125 $\leq$ q $\leq$ 1.75	
f_b	$e = 0.0$	$f(e) = 1.5\sqrt{e}$
0%	0.47	0.48
10%	0.69	0.72
20%	0.88	0.89
25%	0.92	0.92
30%	0.81	0.82
40%	0.46	0.45
50%	0.14	0.16

Figure 1. Spectra showing Number Counts versus Wavelength (Å) for three objects: 1(a) Star LY014 1992, 1(b) Star LY014 1994, and 1(c) M13 Star II−76 Velocity Standard. Labeled features include H$_\beta$ and Mg I triplet.

Histogram of σ_0

ID	RA	DEC (1950)	R (")	HJD (+244000days)	V_r kms^{-1}	σ kms^{-1}	n	$\bar{V}_r$ kms^{-1}	σ kms^{-1}	χ^2	$P(< \chi^2)$	V_0	$(B - V)_0$
S35	13:14:29.803	18:01:17.816	450.4	8719.777	296.7	8.3	5	290.8	3.7	1.239	0.8760	16.69	0.75
				8768.330	291.8	2.4							
				9093.791	286.4	6.4							
				9454.247	290.3	2.0							
				9481.533	290.8	2.3							
LY014	13:14:20.325	18:04:06.804	498.8	8719.777	292.3	3.6	6	291.7	3.5	3.976	0.5528	17.12	0.63
				8768.330	291.3	1.8							
				9093.791	289.2	3.2							
				9128.754	287.6	5.1							
				9454.247	297.7	3.7							
				9481.533	291.9	1.7							
S33	13:14:19.468	17:57:54.244	219.2	9481.533	291.3	1.3	2	291.7	1.2	0.345	0.5572	16.06	0.72
				9454.247	292.8	2.2							
S37	13:14:14.123	18:03:22.185	424.3	9454.247	291.6	1.7	2	291.1	1.1	0.125	0.7242	15.28	0.81
				9481.533	290.8	1.5							
LY019	13:14:13.245	17:58:17.772	153.5	8719.777	285.8	12.4	4	293.6	6.8	1.232	0.7454	18.54	0.65
				8768.330	297.1	7.4							
				9093.791	301.6	11.3							
				9454.247	292.1	4.5							
S38	13:14:11.189	18:01:03.399	279.4	8719.777	291.4	5.0	5	287.6	4.2	3.390	0.4948	17.33	0.60
				8768.330	289.9	4.9							
				9093.791	284.4	8.3							
				9454.247	289.4	3.5							
				9481.533	281.4	4.2							
ST	13:14:26.180	17:58:20.081	318.1	8719.7347	247.9	4.1	14	299.2	40.9	3938	0.0	16.36	0.81
				8719.7769	235.9	3.4							
				8719.8184	252.1	2.9							
				9453.8303	338.1	2.2							
				9453.8850	336.7	2.4							
				9453.9424	337.0	2.2							
				9454.7627	295.6	2.4							
				9454.8137	291.3	2.0							
				9454.8649	287.7	2.6							

Name	Time1	Time2	Val	Freq	Col1	Col2	N	Mean	SD	V1	V2	V3	V4
				9480.6831	337.6	2.0							
				9480.7310	338.7	2.1							
				9480.7857	335.4	2.3							
				9482.7090	254.2	1.7							
				9482.7564	254.7	1.8							
LY116	13:14:11.950	17:57:36.648	114.4	8719.777	289.4	2.5	4	289.7	1.2	0.508	0.9172	17.57	0.63
				8768.330	288.8	2.0							
				9454.247	290.5	3.9							
				9481.533	290.7	2.0							
S45	13:14:10.314	17:58:55.271	156.3	8719.777	292.7	4.2	6	292.4	6.8	5.199	0.3920	16.48	0.68
				8768.330	290.8	3.4							
				9093.791	295.0	3.6							
				9128.754	301.6	4.8							
				9454.247	290.2	3.6							
				9481.533	291.0	2.2							
S41	13:14:09.486	17:59:24.254	177.8	8719.777	289.6	4.0	6	290.0	3.0	1.357	0.9289	16.54	0.74
				8768.330	290.6	3.5							
				9093.791	292.7	4.4							
				9128.754	284.0	6.4							
				9454.247	290.6	3.3							
				9481.533	289.5	2.9							
LY022	13:14:8.497	17:56:40.615	49.0	8719.777	290.5	2.7	5	290.2	1.8	1.282	0.8644	17.49	0.61
				8768.330	292.3	3.2							
				9093.791	291.8	4.1							
				9454.247	288.7	6.9							
				9481.533	288.2	2.5							
S28	13:14:07.689	17:57:10.948	49.8	8719.777	292.2	4.4	5	290.5	3.6	6.224	0.1830	17.04	0.66
				8768.330	294.1	2.2							
				9093.791	285.0	3.2							
				9454.247	289.8	2.8							
				9481.533	288.4	3.4							
S26	13:14:04.983	17:56:53.106	15.2	9454.247	296.4	3.7	2	293.7	3.7	1.054	0.3046	17.01	0.68
				9481.533	291.1	3.6							
S54	13:14:04.168	17:57:53.199	76.3	8719.777	277.1	3.1	6	291.1	9.6	39.236	0.0000	16.63	0.65
				8768.330	292.2	2.2							
				9093.791	295.4	3.2							
				9128.754	281.0	4.7							
				9454.247	294.0	3.4							
				9481.533	302.6	3.4							

LY37	13:14:03.277	17:59:45.181	188.9	9481.533	293.4	5.7	1	293.4	5.7	-	-	18.14	0.56
LY22	13:14:01.636	17:58:15.147	108.8	8719.777	290.1	3.5	3	292.1	3.4	1.110	0.5739	17.60	0.57
				8768.330	294.9	3.6							
				9128.754	288.8	7.8							
LY31	13:14:01.777	18:0:12.363	219.5	9454.247	296.5	6.5	2	290.9	3.4	1.264	0.2609	18.55	0.55
				9481.533	287.0	5.4							
S56	13:14:02.381	17:57:14.604	53.0	9454.247	290.2	2.1	2	291.1	1.6	0.433	0.5104	16.58	0.73
				9481.533	292.4	2.6							
S60	13:14:0.900	17:59:11.026	49.8	8719.777	287.0	2.6	5	291.0	3.8	4.746	0.3143	16.68	0.67
				8768.330	290.9	3.8							
				9093.791	297.2	5.2							
				9454.247	290.5	2.3							
				9481.533	293.1	2.2							
LY28	13:14:0.052	17:59:47.882	202.9	8791.777	293.4	2.8	4	292.5	4.9	1.821	0.6104	17.86	0.65
				8768.330	291.9	4.3							
				9454.247	284.1	6.6							
				9481.533	293.2	2.5							
S66	13:13:59.098	17:59:26.701	189.0	8791.777	288.7	3.7	5	290.5	2.4	1.901	0.7539	16.79	0.67
				8768.330	289.0	3.8							
				9093.791	286.7	4.6							
				9454.247	290.5	3.0							
				9481.533	292.5	2.2							
S84	13:13:57.296	17:58:01.991	139.1	8791.777	293.8	3.2	4	293.0	1.4	0.451	0.9294	15.94	0.72
				8768.330	293.6	2.4							
				9093.791	293.2	2.5							
				9454.247	291.3	3.0							
S90	13:13:57.740	17:56:55.873	106.1	9481.533	289.7	2.8	1	289.7	2.8	-	-	15.98	0.76
LY52	13:13:56.530	17:57:06.575	125.2	9454.247	291.4	4.7	1	291.4	4.7	-	-	17.93	0.61
LY042	13:13:55.074	17:58:18.612	174.6	9481.533	290.7	6.8	1	290.7	6.8	-	-	17.82	0.57
LY043	13:13:54.012	17:58:09.566	182.4	8719.777	287.0	1.7	3	288.2	5.1	2.945	0.2294	17.14	0.60
				8768.330	288.8	3.6							
				9454.247	295.2	4.5							
LY1	13:13:52.698	17:56:28.824	176.8	8719.777	288.7	5.1	4	288.0	4.5	3.716	0.2938	17.19	0.64
				8768.330	293.1	4.0							
				9454.247	288.2	6.4							
				9481.533	288.1	4.1							
S80	13:13:51.521	17:58:41.187	229.3	8719.777	293.4	2.5	6	292.5	3.1	1.674	0.8922	16.95	0.74
				8768.330	290.0	3.6							

				9093.791	295.1	3.8					
				9128.754	286.8	8.0					
				9454.247	293.1	4.3					
				9481.533	291.7	3.1					
LY065	13:13:49.572	17:58:0.164	235.9	8719.777	287.0	9.6	2	295.0	8.5	0.953	0.3290	18.60	0.61
				8768.330	298.0	5.9					
S102	13:13:48.913	17:58:18.160	251.4	9454.247	294.6	3.7	2	290.5	4.9	2.038	0.1534	17.24	0.66
				9481.533	287.8	3.0					
SAH	13:13:48.259	17:59:25.503	292.6	8719.777	288.8	3.4	5	290.0	3.0	2.752	0.6001	17.04	0.59
				8768.330	292.1	2.9					
				9093.791	287.7	2.4					
				9128.754	295.0	4.6					
				9481.533	290.1	1.6					
LY7	13:13:47.502	17:56:52.114	251.1	9454.247	286.6	7.2	1	286.6	7.2	-	-	18.06	0.62
S109	13:13:46.654	17:57:27.460	267.4	8719.777	288.3	3.7	6	297.5	7.6	23.30	0.0003	16.02	0.75
				8768.330	291.6	3.6					
				9093.791	288.6	4.0					
				9128.754	304.9	4.9					
				9454.247	300.2	3.7					
				9481.533	303.2	2.2					
S72	13:13:45.530	18:02:11.898	435.0	9454.247	294.6	0.8	2	294.4	0.6	0.265	0.6068	14.18	1.13
				9481.533	293.9	1.1					
SU	13:13:45.018	17:56:54.485	286.6	8719.777	289.8	4.4	3	293.1	3.9	1.374	0.5031	16.40	0.72
				8768.330	292.8	4.1					
				9093.791	297.5	4.9					
LY004	13:13:43.928	18:02:07.887	447.0	8719.777	289.3	5.9	4	291.1	2.8	1.240	0.7434	17.86	0.61
				8768.330	293.0	2.7					
				9093.791	287.3	5.0					
				9454.247	289.6	5.5					
S108	13:13:45.230	17:57:14.148	285.4	9454.247	292.9	3.4	2	290.1	2.8	0.753	0.3857	16.44	0.72
				9481.533	289.8	1.1					
S106	13:13:35.905	17;57:18.472	418.2	9454.247	301.9	4.8	2	296.9	5.8	1.742	0.1868	17.27	0.58
				9481.533	293.9	3.7					
LY009	13:13:32.497	18:00:17.104	513.9	9481.533	289.0	8.8	1	289.0	8.8	-	-	16.21	0.20
SX	13:14:19.553	17:53:35.426	275.8	8719.777	290.8	3.0	5	291.2	5.0	10.11	0.0386	16.56	0.74
				8768.330	300.9	3.0					
				9093.791	292.0	5.9					
				9454.247	289.9	1.8					

				9481.533	291.0	2.1							
SS	13:14:18.787	17:54:27.594	235.2	8719.777	289.5	2.4	3	291.5	3.1	2.552	0.2791	16.21	0.77
				9454.247	288.2	4.1							
				9481.533	293.7	2.0							
SAB	13:14:16.837	17:53:18.761	260.6	8719.777	291.5	2.9	6	295.1	6.5	16.60	0.0053	16.76	0.66
				8768.330	295.2	2.7							
				9093.791	306.1	4.9							
				9128.754	291.2	9.2							
				9454.247	300.3	2.4							
				9481.533	289.2	2.6							
SP	13:14:13.679	17:56:14.145	125.1	8719.777	292.7	6.2	5	289.1	3.7	3.068	0.5465	15.61	0.80
				8768.330	295.1	4.2							
				9128.754	291.7	4.3							
				9454.247	288.3	1.5							
				9481.533	288.9	1.0							
LY88	13:14:12.704	17:55:37.984	124.4	8719.777	285.2	8.3	3	290.6	5.0	0.987	0.6104	18.65	0.65
				8768.330	286.7	8.0							
				9454.247	283.0	4.2							
S21	13:14:10.278	17:56:18.829	76.8	8719.777	294.7	6.9	3	289.7	4.0	1.254	0.5342	17.18	0.63
				9454.247	287.3	3.1							
				9481.533	290.6	2.5							
S23	13:14:07.463	17:56:08.401	45.2	8719.777	292.2	2.7	5	290.7	2.8	1.591	0.8105	16.40	0.78
				8768.330	288.3	3.7							
				9093.791	289.6	5.1							
				9128.754	295.4	5.6							
				9454.247	290.0	2.1							
SAI	13:14:04.116	17:56:08.155	32.8	8719.777	290.4	4.5	3	288.7	3.5	0.811	0.6668	17.11	0.66
				9454.247	293.2	6.8							
				9481.533	287.5	2.5							
LY17	13:14:03.031	17:52:57.642	222.3	8719.777	288.0	7.4	4	289.9	2.2	0.392	0.9420	18.15	0.62
				8768.330	292.7	6.6							
				9454.247	287.7	5.3							
				9481.533	290.1	2.0							
LY15	13:14:1.653	17:55:18.040	93.7	8719.777	293.9	5.0	4	288.5	6.7	4.654	0.1990	17.32	0.60
				8768.330	298.4	7.1							
				9454.247	286.5	1.8							
				9481.533	290.0	2.7							
S2	13:13:59.996	17:56:13.925	76.3	9454.247	287.9	2.9	2	290.0	3.7	0.507	0.9174	16.04	0.8
				9481.533	289.5	2.0							

S4	13:14:0.241	17:55:17.243	106.2	8719.777	291.4	1.8	4	290.9	3.7	0.507	0.9174	16.81	0.72
				8768.330	289.5	3.5							
				9128.754	284.7	12.0							
				9454.247	290.7	3.2							
LY18	13:13:58.283	17:52:58.351	240.1	8719.777	290.2	6.4	4	291.1	4.6	1.540	0.6730	18.20	0.65
				8768.330	299.0	6.8							
				9454.247	291.6	3.7							
				9481.533	290.2	2.3							
S91	13:13:57.385	17:56:08.211	144.2	8719.777	291.5	4.3	4	296.1	9.4	13.63	0.0035	16.97	0.70
				8768.330	310.9	4.9							
				9454.247	291.8	2.6							
				9481.533	298.4	2.9							
S5	13:13:56.001	17:54:56.196	164.7	8719.777	304.3	2.8	5	295.1	9.9	35.86	0.0000	15.67	0.74
				8768.330	294.5	3.1							
				9093.791	280.3	6.0							
				9454.247	287.5	2.1							
				9481.533	300.9	2.4							
S94	13:13:55.155	17:55:48.676	149.8	8719.777	291.1	2.6	3	290.4	5.1	0.505	0.7768	16.38	0.75
				8768.330	289.8	3.9							
				9128.754	283.3	11.1							
S93	13:13:55.122	17:56:12.750	144.2	9454.247	294.5	2.1	2	295.8	2.4	0.975	0.3235	16.56	0.67
				9481.533	297.8	2.6							
LY85	13:13:54.297	17:51:27.686	346.3	8719.777	293.0	6.2	4	289.0	3.8	0.714	0.8700	18.05	0.65
				8768.330	287.3	5.6							
				9454.247	289.0	5.7							
				9481.533	284.3	11.4							
LY02	13:13:52.945	17:54:47.363	205.4	9454.247	291.8	7.0	2	292.5	3.1	0.013	0.9084	17.58	0.64
				9481.533	292.7	3.4							
LY76	13:13:49.573	17:53:49.279	278.2	9454.247	291.2	6.0	1	291.2	6.0	-	-	17.80	0.62
LY08	13:13:47.715	17:56:17.018	248.5	9454.247	289.7	4.1	2	291.4	4.3	0.588	0.4432	17.57	0.66
				9481.533	295.4	6.2							
LY109	13:13:43.670	17:55:55.426	308.3	9454.247	297.6	5.2	2	293.0	4.8	0.998	0.3178	17.80	0.64
				9481.533	291.7	2.8							
LY015	13:13:43.993	17:52:9.349	403.3	9454.247	290.0	2.3	2	290.7	5.4	0.757	0.3842	17.48	
				9481.533	296.0	6.5							
LY068	13:13:49.262	17:56:14.973	226.8	9454.247	292.5	9.4	1	292.5	9.4	-	-	19.09	0.55
LY03	13:13:52.346	17:55:8.680	202.4	9454.247	289.6	2.1	2	291.2	6.0	2.683	0.1014	17.73	0.55
				9481.533	297.0	4.0							

LY87	13:14:11.701	17:55:26.597	118.5	9454.247	290.5	3.5	2	289.5	3.1	0.315	0.5745	18.32	0.66
				9481.533	286.6	6.0							
LY40	13:14:7.288	17:58:39.484	125.5	9454.247	289.5	3.0	2	290.7	3.6	0.578	0.4469	17.26	0.67
				9481.533	294.0	5.1							
S27	13:14:4.453	17:57:4.988	28.4	9454.247	299.7	4.0	2	294.8	6.3	2.735	0.0982	17.10	0.67
				9481.533	290.8	3.6							
LY65	13:14:3.539	17:56:38.914	21.9	9454.247	285.7	3.0	2	289.0	3.7	1.806	0.1789	17.71	0.59
				9481.533	290.7	2.2							
LY9	13:14:1.330	18:0:48.993	256.6	9454.247	290.2	1.0	1	290.2	1.0	-	-	18.04	0.68
LY11	13:13:59.635	18:0:32.094	246.6	9454.247	289.0	3.7	2	290.1	5.0	0.493	0.4820	17.92	0.66
				9481.533	295.0	7.7							
LY016	13:14:12.485	17:59:59.227	227.4	9454.247	287.7	5.1	1	287.7	5.1	-	-	18.18	0.56
LY017	13:14:13.332	18:2:30.144	371.4	9454.247	294.8	5.0	2	291.0	8.9	1.779	0.1823	18.29	0.55
				9481.533	283.0	7.3							
S70	13:13:57.481	18:0:25.807	252.2	9454.247	289.6	2.8	2	290.8	2.2	0.448	0.5033	17.22	0.65
				9481.533	292.6	3.5							
LYAC	13:13:55.012	17:56:21.794	144.4	9454.247	290.9	3.4	2	289.1	3.3	0.693	0.4050	17.35	0.62
				9481.533	286.4	4.2							
LY13	13:13:51.659	18:0:9.043	284.9	9454.247	292.2	1.1	2	292.1	2.5	0.268	0.6046	17.41	0.70
				9481.533	289.6	5.4							
LY5	13:13:50.600	17:59:2.148	251.8	9454.247	288.6	1.2	2	289.2	1.4	0.692	0.4054	17.45	0.68
				9481.533	290.4	1.8							
LY024	13:13:46.049	18:0:3.952	340.7	9454.247	291.8	6.3	1	291.8	6.3	-	-	18.41	0.60

Notes: See the text for detailed description of the table.

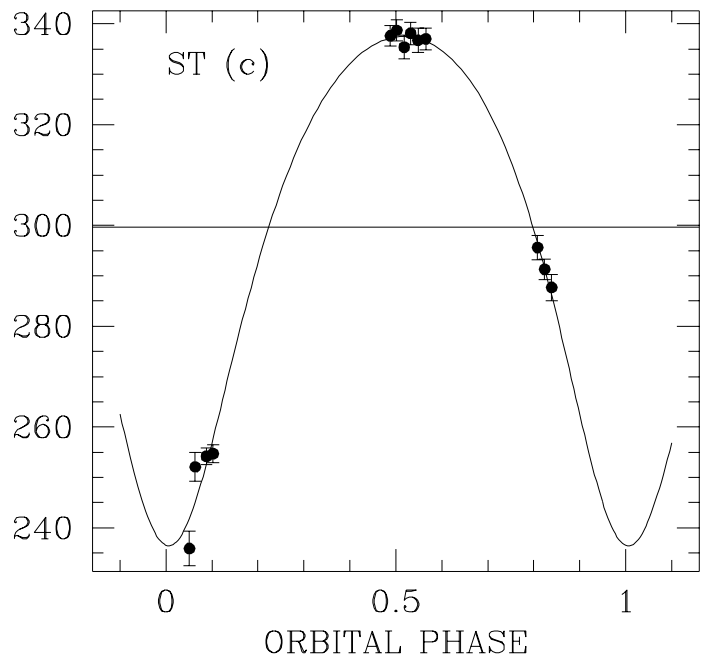Finding Chart for the Binary Candidate ST
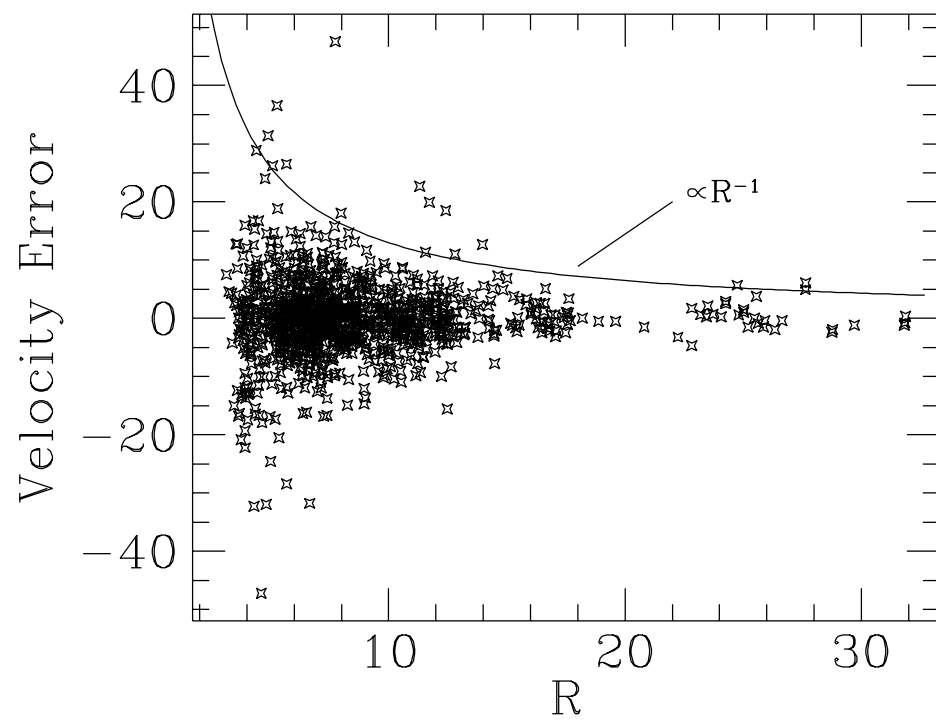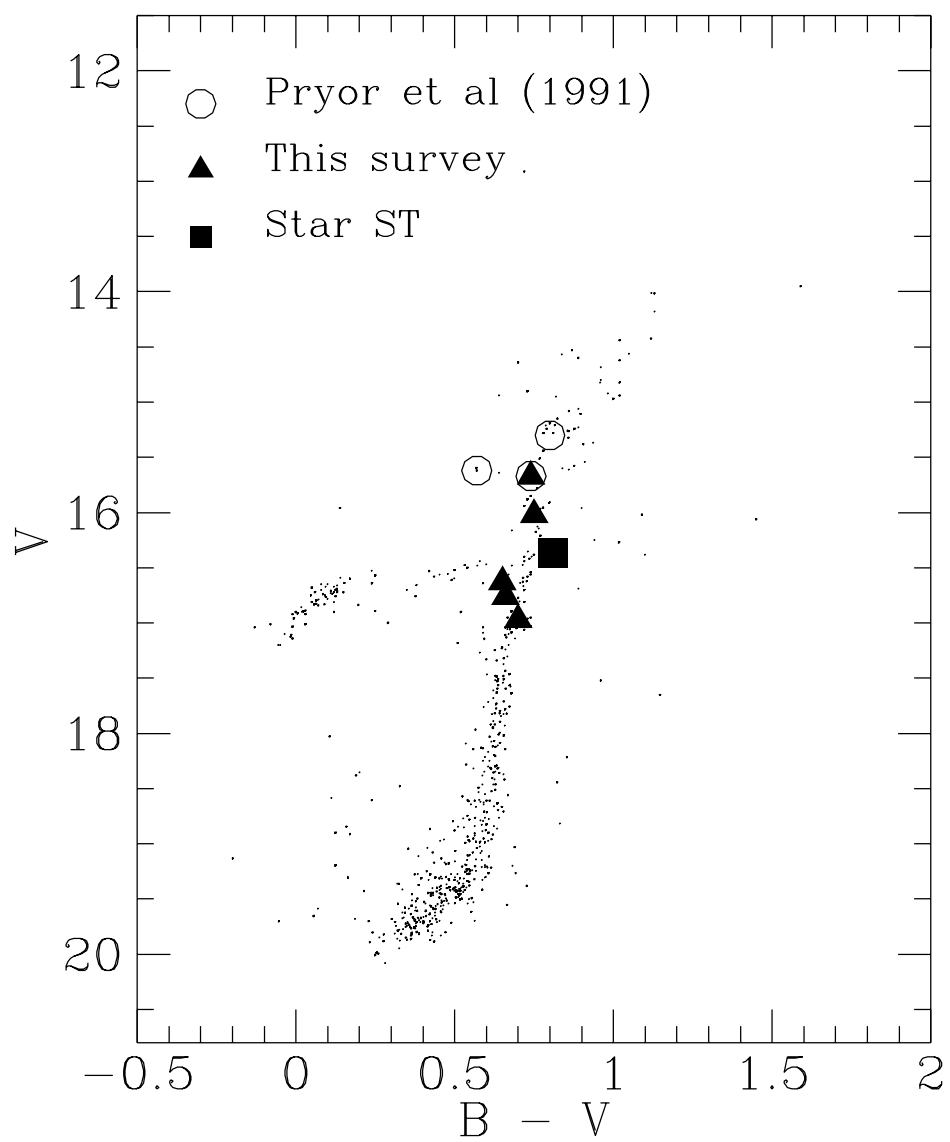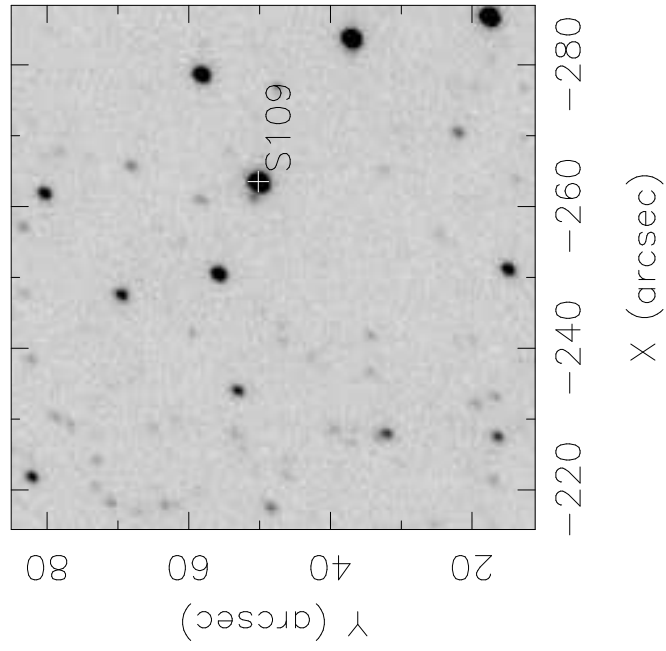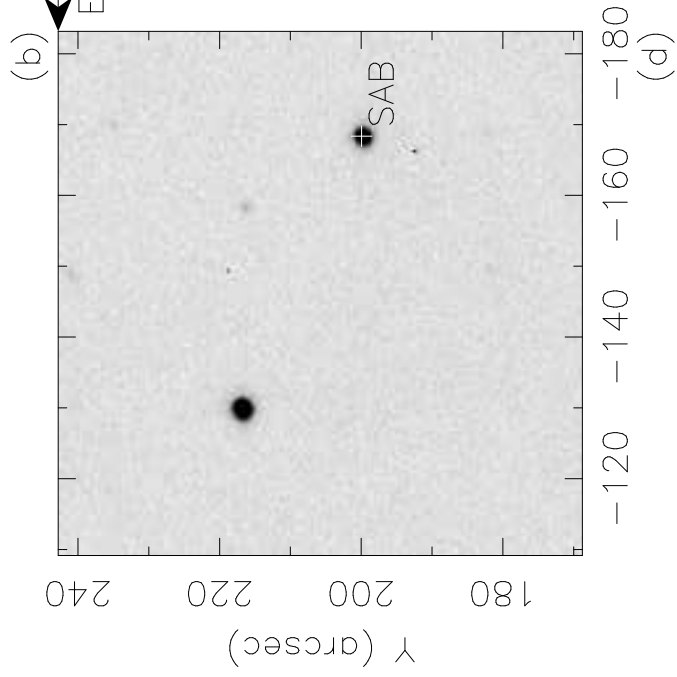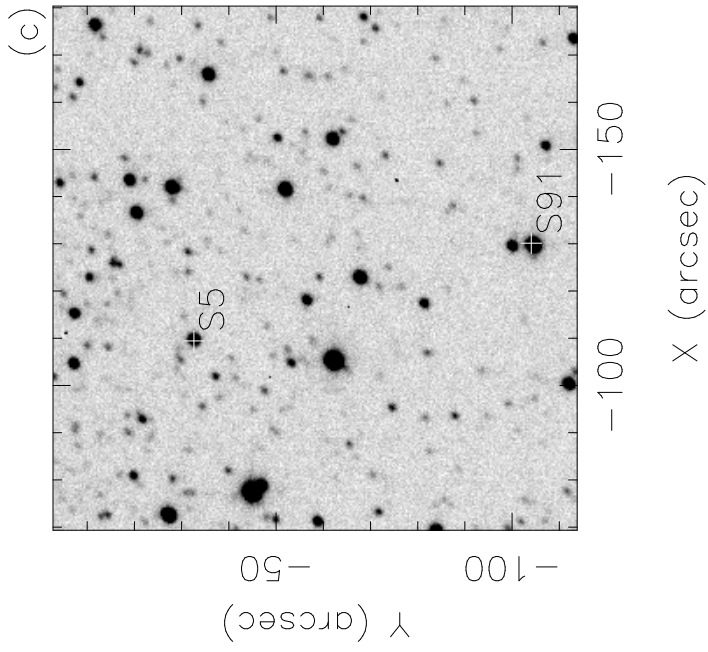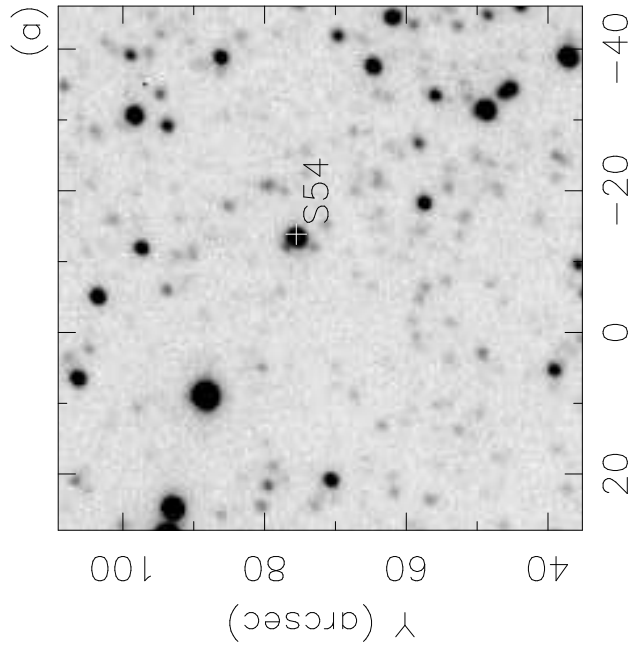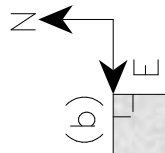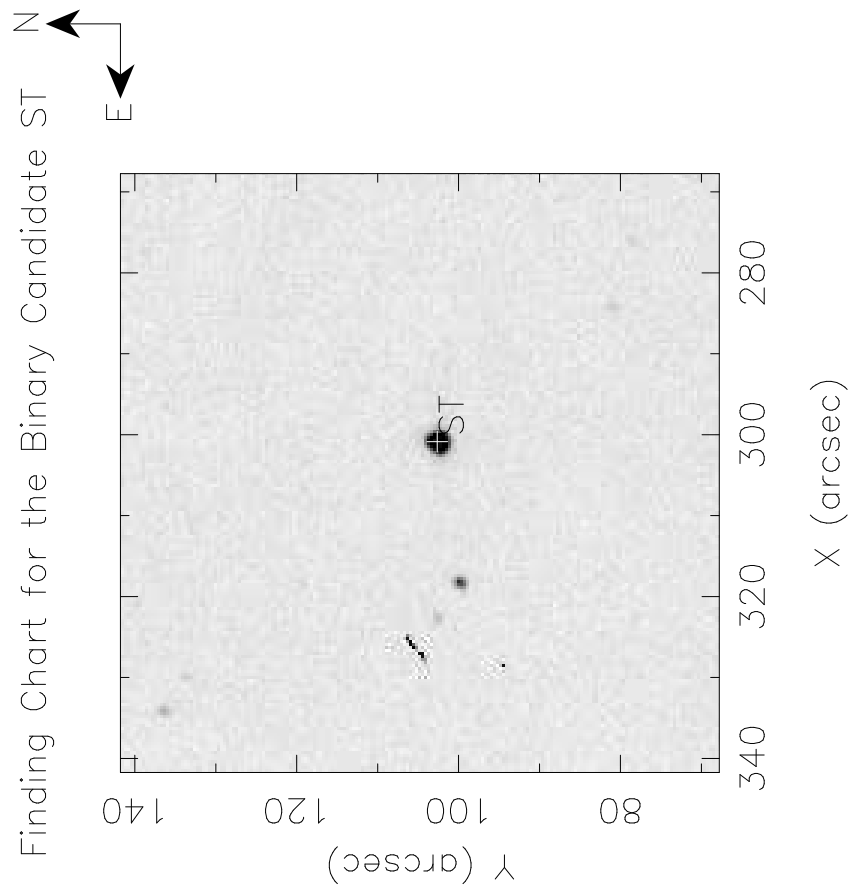
P = 2.979 days, V_0 = 293.52 km s^{-1}
K = 47.5 km s^{-1}, e = 0.191

ST (a)
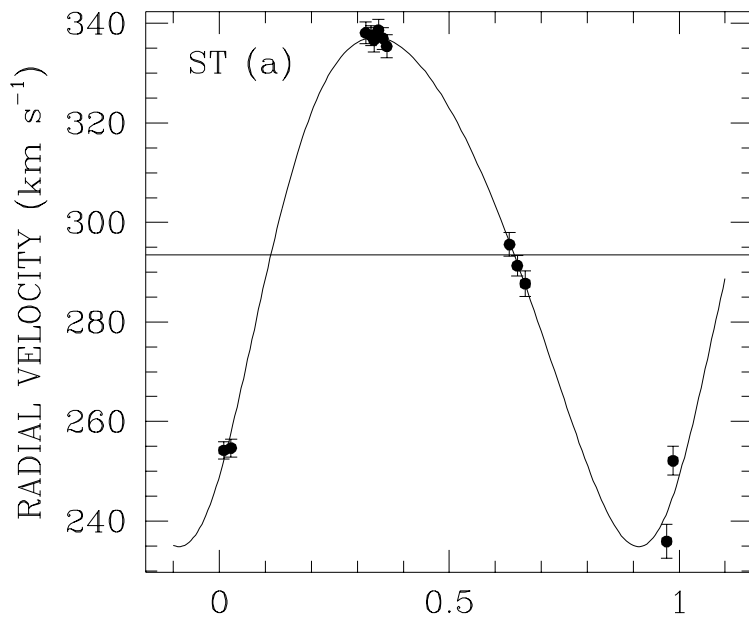
P = 3.8394 days, V_0 = 279.34 km s^{-1}
K = 49.8 km s^{-1}, e = 0.414

ST (b)
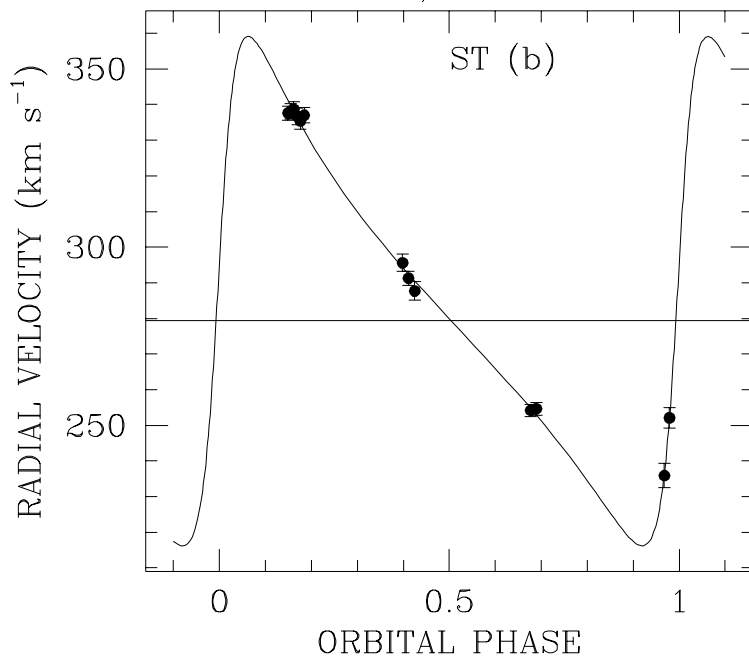
P = 3.3753 days, V_0 = 299.66 km s^{-1}
K = 47.2 km s^{-1}, e = 0.196

ST (c)

RADIAL VELOCITY (km s^{-1})

ORBITAL PHASE
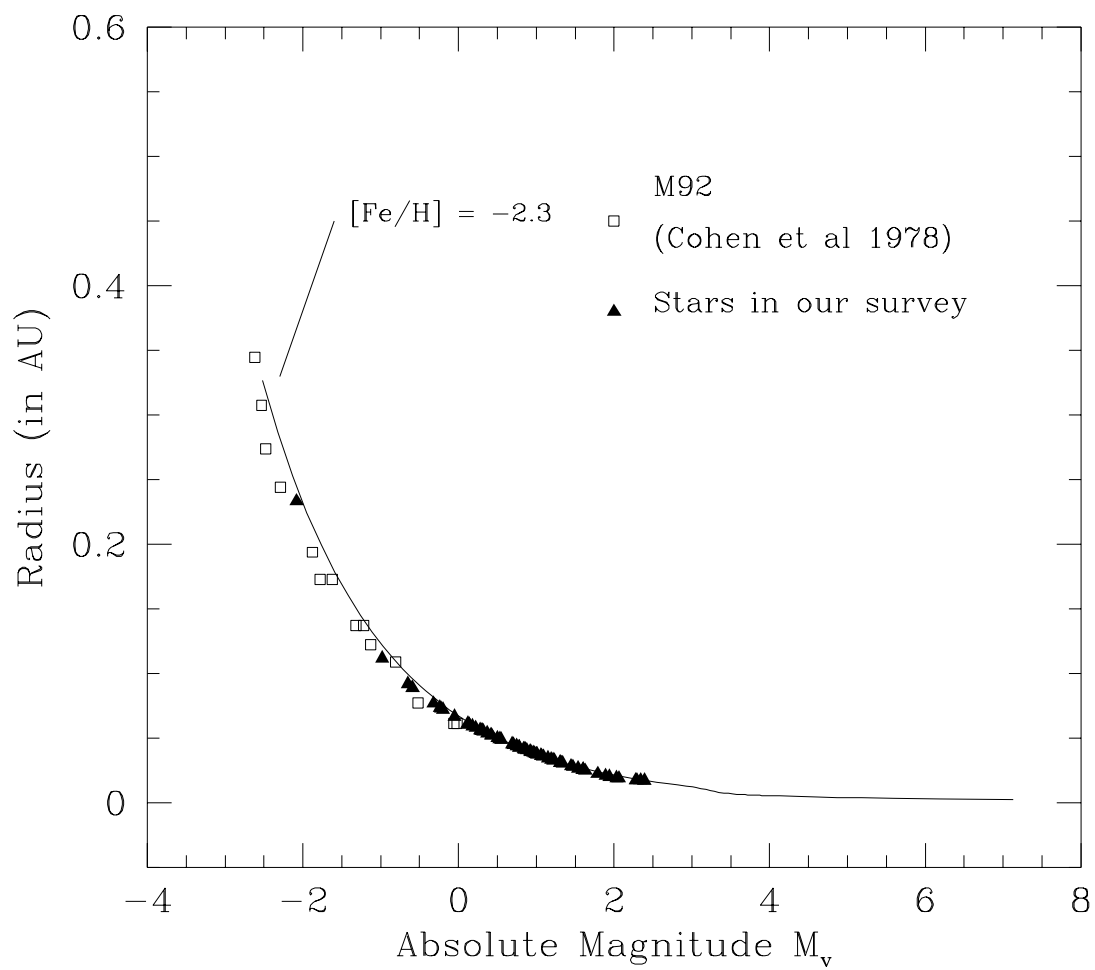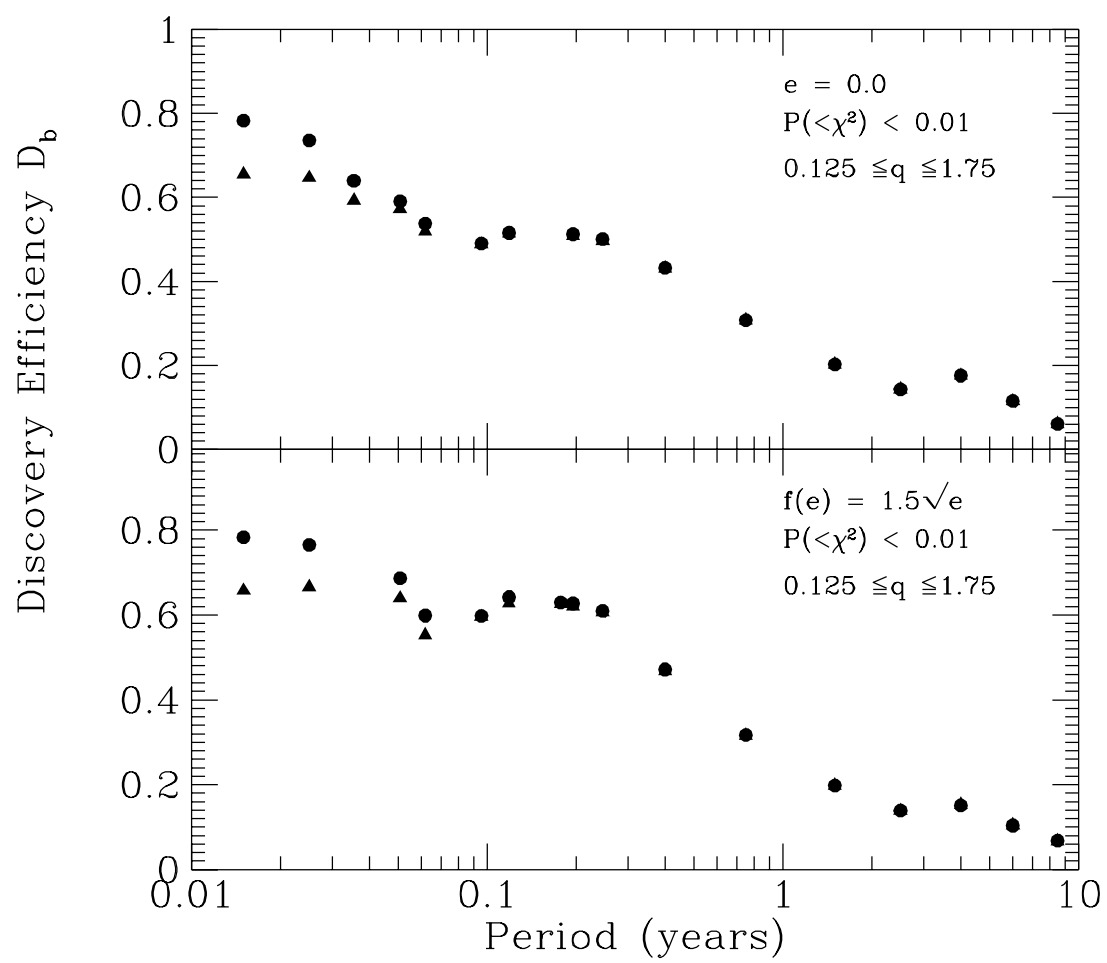
TABLE 3

Spectroscopic Binary Candidates in N5053

ID	HJD (+244000days)	V_r kms^{-1}	σ kms^{-1}	n	$\bar{V}_r$ kms^{-1}	σ kms^{-1}	χ^2	$P(<\chi^2)$	V_0	$(B-V)_0$
S54	8719.777	277.1	3.1	6	291.1	9.6	39.236	0.0000	16.63	0.65
	8768.330	292.2	2.2							
	9093.791	295.4	3.2							
	9128.754	281.0	4.7							
	9454.247	294.0	3.4							
	9481.533	302.6	3.4							
S109	8719.777	288.3	3.7	6	297.5	7.6	23.30	0.0003	16.02	0.75
	8768.330	291.6	3.6							
	9093.791	288.6	4.0							
	9128.754	304.9	4.9							
	9454.247	300.2	3.7							
	9481.533	303.2	2.2							
SAB	8719.777	291.5	2.9	6	295.1	6.5	16.60	0.0053	16.76	0.66
	8768.330	295.2	2.7							
	9093.791	306.1	4.9							
	9128.754	291.2	9.2							
	9454.247	300.3	2.4							
	9481.533	289.2	2.6							
S91	8719.777	291.5	4.3	4	296.1	9.4	13.63	0.0035	16.97	0.70
	8768.330	310.9	4.9							
	9454.247	291.8	2.6							
	9481.533	298.4	2.9							
S5	8719.777	304.3	2.8	5	295.1	9.9	35.86	0.0000	15.67	0.74
	8768.330	294.5	3.1							
	9093.791	280.3	6.0							
	9454.247	287.5	2.1							
	9481.533	300.9	2.4							
ST	8719.7347	247.9	4.1	14	299.2	40.9	3938	0.0	16.36	0.81
	8719.7769	235.9	3.4							
	8719.8184	252.1	2.9							
	9453.8303	338.1	2.2							
	9453.8850	336.7	2.4							
	9453.9424	337.0	2.2							
	9454.7627	295.6	2.4							
	9454.8137	291.3	2.0							
	9454.8649	287.7	2.6							
	9480.6831	337.6	2.0							
	9480.7310	338.7	2.1							
	9480.7857	335.4	2.3							
	9482.7090	254.2	1.7							
	9482.7564	254.7	1.8							

Notes: As in Table 2, see the text for the detailed description of the table.